THE JOURNAL OF BIOLOGICAL CHEMISTRY VOL. 283, NO. 8, pp. 5058–5068, February 22, 2008
Printed in the U.S.A.

Structural and Functional Analysis of the Spt16p N-terminal Domain Reveals Overlapping Roles of yFACT Subunits*[S]

Received for publication, October 19, 2007, and in revised form, December 3, 2007 Published, JBC Papers in Press, December 18, 2007, DOI 10.1074/jbc.M708682200

Andrew P. VanDemark[‡1], Hua Xin[‡], Laura McCullough[‡], Robert Rawlins[‡], Shayla Bentley[§], Annie Heroux[¶], David J. Stillman[§], Christopher P. Hill[‡2], and Tim Formosa[‡3]

From the Departments of [‡]Biochemistry and [§]Pathology, University of Utah School of Medicine, Salt Lake City, Utah 84112 and [¶]Biology Department, Brookhaven National Laboratory, Upton, New York 11973

yFACT (heterodimers of *Saccharomyces cerevisiae* Spt16-Pob3 combined with Nhp6) binds to and alters the properties of nucleosomes. The essential function of yFACT is not disrupted by deletion of the N-terminal domain (NTD) of Spt16 or by mutation of the middle domain of Pob3, but either alteration makes yeast cells sensitive to DNA replication stress. We have determined the structure of the Spt16 NTD and find evidence for a conserved potential peptide-binding site. Pob3-M also contains a putative binding site, and we show that these two sites perform an overlapping essential function. We find that yFACT can bind the N-terminal tails of some histones and that this interaction is important for yFACT-nucleosome binding. However, neither the Spt16 NTD nor a key residue in the putative Pob3-M-binding site was required for interactions with histone N termini or for yFACT-mediated nucleosome reorganization *in vitro*. Instead, both potential binding sites interact functionally with the C-terminal docking domain of the histone H2A. yFACT therefore appears to make multiple contacts with different sites within nucleosomes, and these interactions are partially redundant with one another. The docking domain of H2A is identified as an important participant in maintaining stability during yFACT-mediated nucleosome reorganization, suggesting new models for the mechanism of this activity.

yFACT (yeast facilitator of chromatin transcription or transactions) is a heterodimer of the *Saccharomyces cerevisiae* Spt16 and Pob3 proteins that is assisted *in vivo* and *in vitro* by the high mobility group type B domain DNA-binding protein Nhp6 (1, 2). *In vitro*, yFACT binds to histones (3, 4) and can alter the accessibility of DNA within nucleosomes without hydrolyzing ATP and without repositioning the histone octamer core relative to the DNA (5–7). This activity is different from ATP-dependent chromatin remodeling and has been called nucleosome reorganization (6). yFACT and related FACT complexes from other eukaryotes are needed for both normal regulation of transcription (5, 8–11) and for DNA replication (12–20). Reorganization activity therefore appears to be important in a range of chromatin-based processes, including initiation and elongation of transcription, establishment and maintenance of normal chromatin, and survival during DNA replication stress. Consistent with this broad functional importance, FACT family members have been found in all eukaryotes examined, and at least one of the subunits is essential for viability in all cases reported (9, 21, 19, 22).

FACT complexes contain several distinct structural domains (16, 23), but little is known about how these domains contribute to FACT function. The middle domain of Pob3 (Pob3-M) forms two pleckstrin homology (PH)[4] folds that are closely juxtaposed (23), with highly conserved surface residues forming a patch in a region often associated with binding sites in PH domain proteins (23). Altering this patch caused increased sensitivity to hydroxyurea (HU) (23), a toxin that blocks dNTP synthesis and therefore causes replication stress. This suggests that the Pob3-M domain contributes to a binding interaction that is of increased importance when yeast cells encounter replication stress. Consistent with a role as a protein-binding module, Pob3-M was shown to interact physically and genetically with Rfa1 (23), a subunit of the eukaryotic single-stranded DNA binding factor RPA. yFACT and RPA appear to have overlapping functions in a process that affects nucleosome deposition during DNA replication (23). However, mutations in the conserved putative interaction surface on Pob3-M did not disrupt the yFACT-RPA interaction *in vitro* (23). Pob3-M may therefore have multiple binding partners, with each interaction contributing to different functions of yFACT in different contexts.

The N-terminal domain (NTD) of Spt16 forms an independent structural unit (16, 23). Surprisingly, although this domain is conserved among all known Spt16 homologs, it is not essential for viability in yeast cells, although it is required for normal growth in the presence of high levels of HU (16). The Spt16 NTD shares limited sequence similarity with a class of aminopeptidases, but it does not have peptidase active site residues (see Ref. 24 and this study). These observations suggest that the

* This work was supported by National Institutes of Health grants (to T. F., D. S., and C. P. H.) and an American Cancer Society grant (to A. P. V.). The costs of publication of this article were defrayed in part by the payment of page charges. This article must therefore be hereby marked "*advertisement*" in accordance with 18 U.S.C. Section 1734 solely to indicate this fact.
The atomic coordinates and structure factors (code 3BIP, 3BIQ, 3BIT) have been deposited in the Protein Data Bank, Research Collaboratory for Structural Bioinformatics, Rutgers University, New Brunswick, NJ (http://www.rcsb.org/).
[S] The on-line version of this article (available at http://www.jbc.org) contains supplemental Methods, Figs. S1–S5, and Table S1.

[1] Present address: Dept. of Biological Sciences, University of Pittsburgh, Pittsburgh, PA 15260.
[2] To whom correspondence may be addressed. Tel.: 801-585-5536; Fax: 801-581-7959; E-mail: chris@biochem.utah.edu.
[3] To whom correspondence may be addressed. Tel.: 801-581-5435; Fax: 801-581-7959; E-mail: tim@biochem.utah.edu.

[4] The abbreviations used are: PH, pleckstrin homology; WT, wild type; HU, hydroxyurea; NTD, N-terminal domain; TEV, tobacco etch virus; PDB, Protein Data Bank; 5-FOA, 5-fluoroorotic acid.

Spt16 NTD may have peptide binding activity but that this role is dispensable for the core activity of yFACT.

Here we report the structure of the Spt16 NTD and the results of studies examining the role of this domain in yFACT function. The Spt16 NTD is structurally similar to aminopeptidases, and the most highly conserved surface residues line a cleft equivalent to the aminopeptidase substrate-binding site. The presence of potential peptide-binding sites in each subunit of yFACT led us to examine candidate substrates, initially focusing on the attractive possibility that these sites bind to the N-terminal tails of histones that extend beyond the structured core of the nucleosome and are known to influence yFACT functions *in* vivo (6, 25). The N-terminal tails of histones were found to have an important role in yFACT function and to be bound by yFACT with high affinity. However, this activity and other measurable functions of yFACT *in vitro* remained intact after mutating Pob3-M or deleting the Spt16 NTD. Instead, the Spt16 NTD and Pob3-M domains were found to have overlapping roles in a process that involves the C-terminal extension of H2A. This stirrup-like "docking domain" of histone H2A acts to stabilize the binding of H2A-H2B dimers to $(H3\text{-}H4)_2$ tetramers within histone octamers (26–28). These results suggest that yFACT makes multiple additive contacts with nucleosomes during reorganization, and that some of these contacts are important after yFACT has induced the reorganization of the nucleosome. The docking domain of H2A is identified as an important contributor to this process, perhaps tethering nucleosomal components together or controlling the insertion of H2A-H2B dimers during nucleosome formation.

EXPERIMENTAL PROCEDURES

Protein Expression and Purification—DNA fragments encoding Spt16 residues 1–451 or 1–465 were amplified by PCR and inserted into a modified pET bacterial expression vector that fused eight histidines and a TEV protease site to the N termini. TEV cleavage leaves the sequence "GHM . . . " at the N terminus in place of the native methionine. Each protein was expressed in Codon+(RIL) cells (Stratagene) and purified by nickel chelation chromatography (Qiagen). After TEV protease digestion and nickel chelation chromatography to remove tagged N termini, proteins were further purified by gel filtration on Superdex-200 (GE Healthcare) in 10 mM HEPES, pH 7.5, 150 mM NaCl, 2% glycerol, 1 mM 2-mercaptoethanol. The Spt16 NTD fragments eluted as apparent monomers and were then concentrated in gel filtration buffer.

Spt16-Pob3 complexes with 12 histidines and a TEV site fused to the N terminus of Pob3 were purified from yeast cells overexpressing each protein from the *Gal1* promoter after growth in galactose medium, as described (19). Complexes were purified from extracts using nickel chelation and gel filtration as above, except using Sephacryl S300 (GE Healthcare) and omitting the TEV cleavage.

Nucleosomes were prepared by dialysis from high ionic strength solutions using derivatives of a sea urchin rDNA nucleosome positioning sequence and chicken histones or bacterially expressed yeast histones, as described previously (7; see the supplement material for details).

Crystallography—Single plate crystals of Spt16-(1–451) were grown at 4 °C over 2–3 weeks by sitting drop vapor diffusion against a reservoir solution of 200 mM NaCl, 100 mM sodium acetate, pH 4.5, and 35% polyethylene glycol 300. The drop consisted of 1 μl of protein concentrated to 10–15 mg/ml, 1 μl of reservoir solution, and 0.4 μl of 100 mM cysteine. Selenomethionine-substituted Spt16-(1–451) was expressed as described (29) and then purified and crystallized using conditions similar to those described above. Crystals were cryoprotected by emersion in reservoir solution made up with 25% glycerol and then flash-frozen in liquid nitrogen. SAD data were collected at National Synchrotron Light Source beamline X26-C and processed with HKL2000 and SCALEPACK (30). Nine of the 10 possible selenium positions in the two molecules in the asymmetric unit were located by SOLVE (31), and an initial model was built into the experimental electron density maps using RESOLVE (32).

Two visually indistinguishable but distinct crystal forms (space groups P1 and $P2_1$) of native Spt16-(1–465) were grown overnight at 22 °C from a single drop with 1.2 μl of 14 mg/ml protein solution, 1.2 μl of reservoir solution, and 0.4 μl pentanediol by vapor diffusion against a reservoir solution of 25% pentaerythritol ethoxylate (15/4 EO/OH) and 100 mM sodium acetate, pH 4.5. Data were collected and processed as above. The refined model of Spt16-(1–451) was used as a starting model for molecular replacement (PHASER; 33) into both native datasets. Model building for all structures reported here was performed using COOT (34). Refinement used REFMAC implemented within CCP4i (35), and the TLSMD server to generate TLS parameters (36). The structures have been deposited into the Protein Data Bank under the codes 3BIP, 3BIQ, and 3BIT.

Genetic Methods—Strains used are described in supplemental Table S1. Standard yeast methods and media were as described (37).

RESULTS

Structure of the Spt16 NTD—The boundaries of the Spt16 NTD were determined as described previously (16, 23), and soluble fragments, including residues 1–451 and 1–465, were expressed and crystallized. Experimental phases were determined by the SAD method using selenomethionine-substituted protein, and the model was refined to R_{factor}/R_{free} values of 18.0/22.3% against data to 1.9 Å resolution (crystallographic statistics are given in Table 1). This model was used in molecular replacement calculations to determine two different crystal forms of native Spt16 NTD that were refined to R_{factor}/R_{free} values of 17.6/24.4% and 15.1/21.0% against data to 1.94 and 1.75 Å resolution, respectively. The five independent Spt16 NTD molecules in these three crystal forms displayed only minor differences, with a maximum root mean square deviation of 0.7 Å for overlap on 440 pairs of C-α atoms in pairwise comparisons.

Comparison with Other Structures—The Spt16 NTD includes a smaller N-terminal lobe (residues 1–175) and a larger C-terminal lobe (residues 176–447; Fig. 1). The extensive packing between the lobes and the similarity of crystallographically independent molecules suggest that the two lobes maintain a fixed relative orientation in solution. The N-termi-

TABLE 1

Data collection and refinement statistics

Values in parentheses correspond to those in the outer resolution shell.

	Native form I	Native form II	Selenomethionine form III
Data collection			
Space group	P1	$P2_1$	$P2_1$
Cell dimensions (Å)	a = 51.1, b = 60.1, c = 85.9	a = 60.3, b = 50.8, c = 79.2	a = 40.7, b = 144.6, c = 88.5
Unit cell angles (°)	$\alpha = 72.6$, $\beta = 77.1$, $\gamma = 89.9$	$\beta = 107.1$	$\beta = 101.4$
Resolution (Å)	50-1.94	50-1.75	40-1.90
Detector edge shell (Å)[a]	2.44-2.30	2.38-2.20	
Resolution outer shell (Å)	2.01-1.95	1.81-1.75	1.97-1.90
No. of observations	361,089	522,903	3,070,941
No. of unique reflections	51,635	33,504	73,990
R_{sym} (%)[b]	7.2 (40.7)	10.2 (32.6)	9.6 (45.2)
$I/\sigma(I)$	22.5 (3.1)	15.7 (2.4)	20.3 (2.4)
Completeness to detector edge (%)	93.2	98.4	
Completeness to outer shell (%)	73.1 (24.9)	71.8 (12.4)	94.0 (69.6)
Refinement			
R_{work}/R_{free} (%)[c,d]	17.6/24.4	15.1/21.0	18.0/22.3
No. of atoms			
Protein	7,321	3,643	7,396
Solvent	732	422	1,045
Average isotropic B-factor(Å)^2	26.3	29.4	40.7
Ramachandran plot (non-Gly)			
Most favorable region (%)	91.6	91.3	91.6
Allowed region (%)	8.3	8.7	8.4
Generous allowed region (%)	0.1	0.0	0.0
Disallowed region (%)	0.0	0.0	0.0
Root mean square deviations			
Bond lengths (Å)	0.011	0.012	0.016
Bond angles (°)	1.346	1.314	1.465

[a] Detector edge outer shell represents the bin of data that extended to the edge of the detector. Upon reexamination of the data, it was found that quality data could be obtained in the corner of the diffraction images. The added data were of high quality but limited in completeness; therefore, we report completeness statistics both to the detector edge and including the higher resolution data. The higher resolution data were included throughout structure refinement, and refinement statistics (including R values) were calculated using all the data.

[b] $R_{sym} = (|(\Sigma I - \langle I \rangle|)/(\Sigma I)$, where $\langle I \rangle$ is the average intensity of multiple measurements.

[c] $R_{work} = \Sigma||F_{obs}| - |F_{calc}||/\Sigma|F_{obs}|$

[d] R_{free} = the cross-validation R factor for 5% of reflections against which the model was not refined.

nal lobe structure is similar to the RuvC/RNase H family, with a root mean square deviation of 3.3 Å for overlap with RuvC (38; PDB 1HJR) over 89 pairs of C-α atoms (supplemental Fig. S1). Structures in this family include a 3-layer $\alpha/\beta/\alpha$ sandwich in which the central β-sheet is composed of five strands (order 32145) that, with the exception of strand 2, are parallel to each other. The RuvC active site is formed by a cluster of four acidic residues that lie in a deep cleft formed by both the β-sheet and the helical regions on one side of the sheet. The Spt16 NTD lacks these catalytic residues and contains an additional helix (residues 36–62) that fills this cleft. Furthermore, the charged nucleic acid binding surface of RuvC and RNase H is not conserved in the Spt16 NTD. The limited structural similarity therefore does not indicate a shared biochemical activity of Spt16 with RuvC/RNase H, consistent with the earlier finding that yFACT does not bind DNA in affinity purification or electrophoretic mobility shift experiments (6, 19).

The Spt16 NTD C-terminal lobe adopts a "pita bread" fold, in which two $\alpha\alpha\beta\beta\beta$ motifs associate with approximate 2-fold symmetry to form a half-barrel structure (Fig. 1). This architecture is also found in the aminopeptidases that share limited sequence similarity with the Spt16 NTD, including methionine aminopeptidase, prolidase, and aminopeptidase P. Other structurally similar proteins include creatinase (39, 40) and the ErbB-3 receptor-binding protein (Ebp1; 41, 42). The C-terminal lobe shows closest structural similarity to the prolidase enzyme from *Pyrococcus furiosus* (PDB 1PV9; 43), which overlaps with a root mean square deviation of 2.0 Å over 215 pairs of C-α atoms that share 23% sequence identity (Fig. 2).

The cleft formed at the open side of the half β-barrel in enzymes with a pita bread fold is often found to house the active site. The Spt16 NTD displays a cleft at this position that measures ~22 × 20 Å and is ~10 Å deep. A portion of this cleft is loosely covered by a loop (residues 267–276), forming a short tunnel or covered region within the cleft (*orange* in Figs. 1 and 2). Surface residues that are evolutionarily conserved among Spt16 homologs cluster within the tunnel region and the adjacent section of the cleft (see Fig. 5 below), suggesting that this region is functionally important in Spt16.

Prolidase, methionine aminopeptidase, and aminopeptidase P are peptidases that cleave Xaa-Pro dipeptides, Met-Xaa, and Xaa-Pro peptides, respectively. Consistent with the related chemistry, their active sites are similar structures that feature a dinuclear metal ion cluster. Creatinases are also hydrolases that cleave a C–N bond, although in this case creatine is cleaved to sarcosine and urea. Notably, although ligand complex structures demonstrate that the creatinase and peptidase active sites overlap spatially (Fig. 2), creatinase uses a histidine side chain rather than coordinated metal ions to drive catalysis. Spt16 does not contain either the metal ion coordinating residues of the peptidases or the histidine of creatinase. Additionally, yFACT purified from yeast cells was not found to contain metal atoms,[5] and neither yFACT nor the Spt16 NTD displayed peptidase activity with a variety of substrates (see supplemental material).[6] We therefore disfavor the model that Spt16 NTD is

[5] D. Winge, University of Utah, personal communication.

[6] M. Rechsteiner, University of Utah, personal communication.

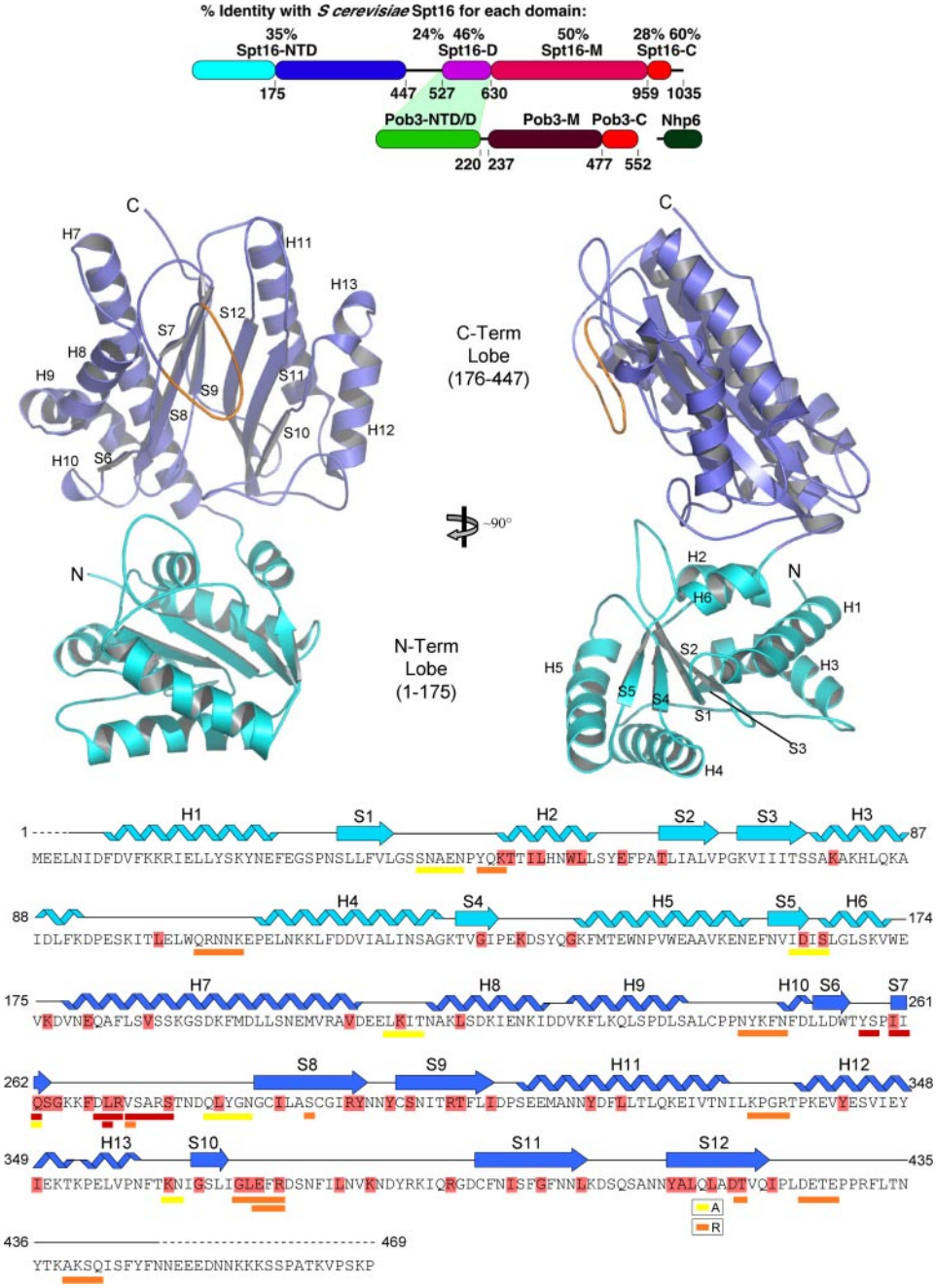

FIGURE 1. **Structure of the Spt16 NTD.** *Top,* the residues in each structural domain of Spt16-Pob3 are indicated (16, 23). 31 Spt16 homologs chosen to include the full spectrum of eukaryotes were aligned and found to be about 40% identical to the yeast sequence overall. The percent identity to the *S. cerevisiae* sequence varied for each domain as indicated. All homologs included the NTD. The C-terminal domain is broken into two regions for this calculation, a less conserved but 50% acidic region (960–1008) and a more highly conserved and neutral region (1009–1029). *D* indicates the dimerization interface. *Middle,* ribbon diagrams of the Spt16 NTD structure. The N-terminal lobe is shown in *turquoise*; the C-terminal lobe containing the putative binding cleft in *blue*, and the loop that encloses the cleft in *orange*. Labels indicate the secondary structure features. *Bottom,* secondary structures within the Spt16 NTD are aligned with the sequence. Residues that are conserved among over 70% of the 31 Spt16 homologs compared are highlighted in *red*. *Bars* below the text indicate regions targeted for site-directed mutagenesis, coded according to the severity of the synthetic defect with *pob3-Q308K* (Table 2).

an enzyme, although the remarkable divergence of the peptidase and creatinase active sites cautions that this possibility cannot be completely discounted. Our preferred hypothesis is that the Spt16 NTD groove is a binding site, perhaps for a peptide ligand from a nucleosome or other associated protein. Like the Spt16 NTD, the pita bread fold domain of Ebp1 appears to lack enzymatic activity but retains a distinctive cleft that might function as a binding site (41, 42).

The structural similarity with prolidase and aminopeptidase P is not limited to the Spt16 NTD C-terminal lobe but also extends over the N-terminal lobe. In these peptidases, the N-terminal lobe mediates oligomerization (forming tetramers of aminopeptidase P and dimers of prolidase; see 43). Despite the structural similarity, it seems unlikely that the Spt16 NTD promotes analogous self-association because relevant interactions are not seen in the crystal structures; analytical ultracentrifugation shows that yFACT is a heterodimer of 1:1 stoichiometry (19); the Spt16 NTD is not required for the interaction between Spt16 and Pob3 (16, 23 and see below); and both analytical ultracentrifugation and gel filtration indicate that the isolated Spt16 NTD fragment is a monomer even at very high protein concentrations (not shown). Notably, although monomeric aminopeptidases exist that are missing the N-terminal lobe (methionine aminopeptidase, for example; PDB 1MAT, see Ref. 44), no Spt16 homologs lacking the N-terminal lobe have been identified. The N-terminal lobe of Spt16 may therefore act as a protein-protein interaction domain but presumably with partners outside of the yFACT complex.

Functional Overlap between the Spt16 NTD and Pob3-M—Although the NTD represents 43% of the *SPT16* gene, and deletion of the entire gene is lethal (9), yeast cells survive deletion of residues 2–484 (16). We confirmed this result in different genetic backgrounds by constructing a genomic deletion allele that removes residues 2–468 but causes no other alteration of the genome. Strains with this allele of *SPT16* (*spt16-ΔNTD*) grew normally under a variety of conditions, although they displayed a moderate retardation of growth when exposed to high concentrations of HU, a toxin that causes DNA replication stress by inhibiting deoxynucleotide synthesis (supplemental Fig. S2). Screens for additional phenotypes caused by deletion of the NTD revealed only weak effects (supplemental material). Nota-

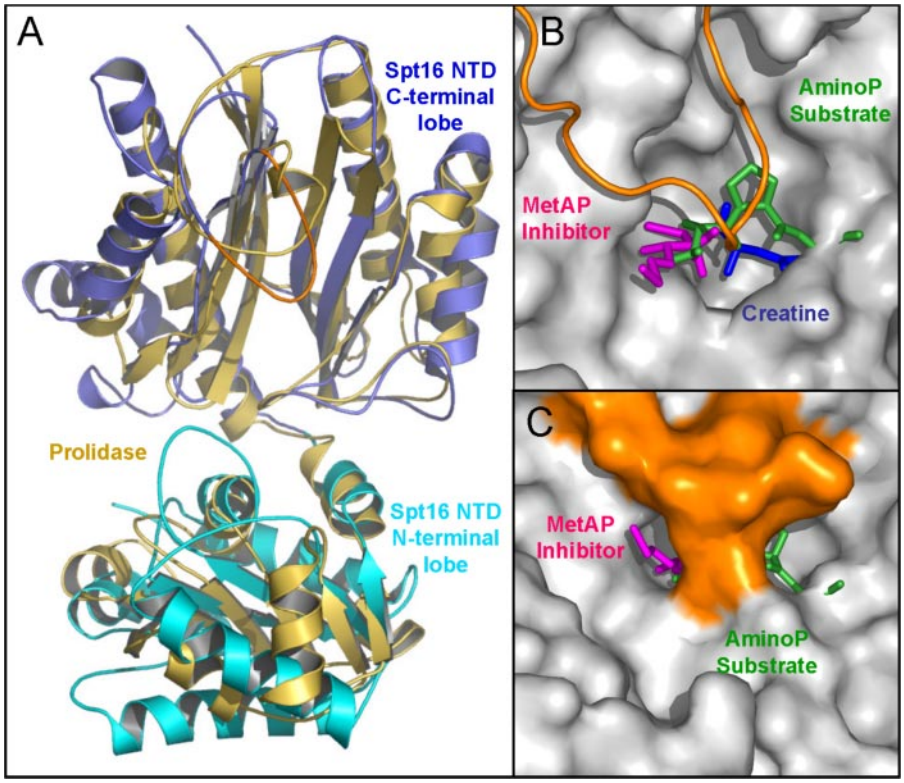

FIGURE 2. **The Spt16 NTD aligns with other pita bread fold proteins.** *A,* Spt16 NTD (*turquoise* and *blue*) is superimposed with prolidase (*yellow*). The loop of Spt16 that encloses the putative binding cleft is colored *orange*. *B* and *C,* a peptide substrate in aminopeptidase P (*AminoP*) (*green*), an inhibitor of methionine aminopeptidase (*MetAP*) (*pink*), and the substrate creatine in creatinase (*blue*) are superimposed on the Spt16 NTD structure. The surface of the loop is omitted in *B* and included in *C* to view different aspects of the tunnel and cleft.

bly, the strains were able to grow normally at elevated temperatures and displayed only a very weak Spt$^-$ phenotype (Fig. 3; the Spt$^-$ phenotype is assayed here as growth on media lacking lysine because of use of aberrant transcription initiation sites within the *lys2-128∂* allele; see Ref. 45). This shows that deletion of the NTD does not destabilize the protein significantly and leaves yFACT able to perform its role in regulating transcription initiation site selection normally. The stability of the Spt16-ΔNTD protein was also confirmed by Western blotting (supplemental Fig. S4). The Spt16 NTD is therefore dispensable under normal laboratory growth conditions but provides a significant selective advantage in some contexts.

Pob3-M forms a double-PH fold with invariant residues clustered at a potential binding surface (23). A Q308K substitution within this surface leads to a stably folded Pob3 protein, but causes sensitivity to high levels of HU and a strong Spt$^-$ phenotype (23) (Fig. 3). These phenotypes show that the normal features of this putative binding pocket on the surface of the Pob3-M domain are needed during replication stress and during transcription. Because *spt16-ΔNTD* and *pob3-Q308K* mutations each affected potential peptide-binding sites, we examined double mutants to see if they affected redundant functions. Double mutants in the W303 genetic background required a plasmid with the WT version of *SPT16* for survival (Fig. 3), indicating that the combination of mutations is lethal. The Spt16 NTD and Pob3-M domains are therefore at least partially redundant for providing an essential function.

Functional overlap between the Spt16 NTD and Pob3-M was also observed in strains from the A364a genetic background, although in this case the double mutant was weakly viable, allowing the defect to be examined more carefully (Fig. 3*B*). Double mutants in A364a displayed a growth defect at all temperatures, inviability at elevated temperatures, and the inability to tolerate even very low levels of HU (Fig. 3*B*). The Spt$^-$ phenotype caused by *pob3-Q308K* was not altered by the loss of the Spt16 NTD, consistent with previous data showing that transcriptional regulation is not significantly affected by deletion of the Spt16 NTD (16).

Although we favor the interpretation that the synthetic defect caused by combining *spt16-ΔNTD* and *pob3-Q308K* mutations is because of loss of redundant functions, an alternative explanation is that the Spt16 NTD and Pob3-M domains interact with one another in a way that stabilizes the proteins. The isolated Spt16 NTD and Pob3-M did not copurify when expressed together (16, 23), and no interaction was detected between the fragments by equilibrium sedimentation (not shown). Furthermore, we found that the Spt16-ΔNTD fragment forms a stable heterodimer with Pob3-Q308K protein even in yeast cells shifted to 37 °C for several hours (see below and supplemental Fig. S4). We therefore conclude that the double mutant yFACT complex Spt16-ΔNTD-Pob3-Q308K lacks an important activity but is structurally intact and stable.

Point Mutations Reveal Functional Overlap of the Spt16 NTD Cleft with Pob3-M—We used site-directed mutagenesis to examine the importance of specific residues in the function of the Spt16 NTD, focusing on surface residues to avoid destabilization of the structure (Table 2). A strain with the entire *SPT16* locus deleted from the genome was constructed and kept alive with a plasmid carrying *SPT16* and *URA3* genes. Mutations in *SPT16* were introduced into a low copy plasmid marked with *LEU2*; transformants with both WT and mutated plasmids were obtained, and strains with only the mutated *SPT16* gene were derived by selection on medium containing 5-FOA, which is toxic to cells with the *URA3* gene (46). Most of the mutations had no effect on growth under the conditions tested, although some caused a mild Spt$^-$ phenotype (Table 2 and supplemental Fig. S3). In particular, the substitutions of surface residues did not cause temperature sensitivity and did not significantly destabilize the Spt16 protein as assayed by Western blotting (supplemental Fig. S4; consistent with previous reports, mutations that perturb the hydrophobic core of the

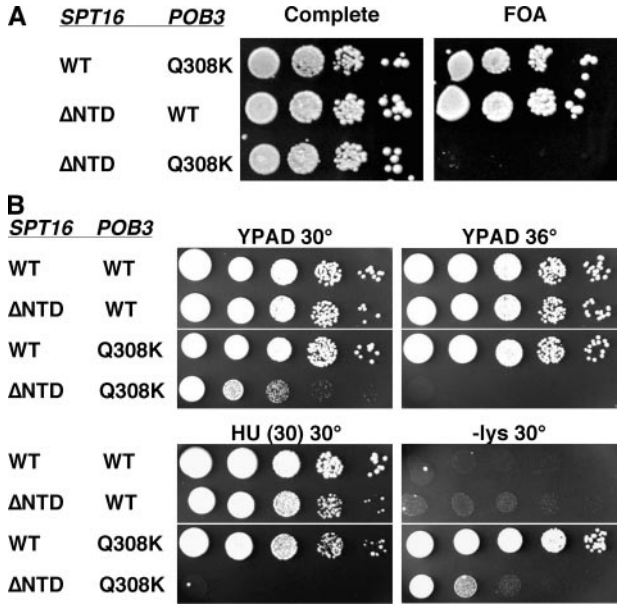

FIGURE 3. **Simultaneous deletion of the Spt16 NTD and mutation of Pob3-M causes a severe synthetic defect.** *A,* strains DY10890, DY11923, and DY12431 (W303 background) with the genotypes indicated and carrying a low copy plasmid with the *POB3* and *URA3* genes were grown to saturation in rich medium. Aliquots of 10-fold dilutions were spotted to complete synthetic medium or medium containing 5-FOA and incubated at 25 °C. Only strains that lose the *URA3* plasmid during nonselective growth are able to grow on plates containing 5-FOA, so lack of growth in the *3rd row* indicates that double mutants are inviable. *B,* strains 8277-26-1, 8137-10-3, 8151-1-2, and 8289-2-4 (A364a background) with the genotypes noted were diluted and tested as indicated. YPAD is rich medium, HU (30) is YPAD with 30 mM hydroxyurea, −lys is synthetic medium lacking lysine (reporting the Spt$^-$ phenotype). Slow growth of the double mutant in the *bottom row* on −lys reflects the slow growth of this strain even on rich medium, not an altered Spt$^-$ phenotype (compare with the same strain on YPAD at 30 °C).

Spt16 NTD did cause both temperature sensitivity and destabilization of Spt16 protein). Furthermore, none of the point mutations that alter surface residues resulted in sensitivity to HU.

We next examined the point mutants to determine which features of the NTD are important for the functional overlap with the Pob3-M domain. A strain with a deletion of *SPT16* and also carrying the *pob3-Q308K* allele was constructed and transformed with the same series of *SPT16* plasmids described above. In this case, a subset of the mutated plasmids was unable to support robust growth on medium containing 5-FOA (Fig. 4*A*), indicating that mutations such as Spt16-IIQ260DIR significantly blocked the function of the Spt16 NTD that overlaps with Pob3-M (alleles with multiple changes are given as the WT sequence, the number of the first affected residue, and the mutated sequence with changes underlined). Most of the *SPT16* alleles tested supported normal growth on rich medium when combined with *pob3-Q308K*, but some of the resulting strains displayed extreme sensitivity to even mildly elevated temperatures or low levels of HU. For example, a *pob3-Q308K* strain with the Spt16-YS257DD plasmid failed to grow at 36 °C or in the presence of 30 mM HU (Fig. 4*B*, *4th row*), conditions that did not affect either single mutant. Tyr-257 and Ser-258 protrude into the Spt16 NTD cleft near the tunnel (Fig. 5). Other mutations such as the triple change QLYGN 279 DLDGR had little or no additive effect with *pob3-Q308K* (Fig. 4*B*). These residues map to the upper portion of the C-terminal lobe of the Spt16 NTD away from the cleft (Fig. 5). Key results obtained from this plasmid-based screen were confirmed by integrating mutations into the genome, and some complex mutations were

TABLE 2

Phenotypes caused by site-directed mutations in the Spt16 NTD

The sequences indicated in the 1st column were mutated to those in the 3rd column by site-directed mutagenesis within a full-length low copy *SPT16* plasmid with the native promoter. The derivatives were shuffled into 7784-1-1 pTF125 (*spt16-*Δ) with the *SPT16* locus deleted from the genome, and then the resulting strains were tested for the ability to grow when challenged with 200 mM HU, incubation at 37 °C, or on media lacking histidine or lysine (the Spt$^-$ phenotype). Some isolates had a moderate Spt$^-$ phenotype, but none displayed sensitivity to HU or elevated temperatures. The screen was repeated in 8319-2-4 (*spt16-*Δ *pob3-Q308K*) using 6, 15, 30, and 60 mM HU, 30, 33, 36, and 37 °C, and media lacking lysine. Dilutions were tested as shown in Fig. 4 and then rated from 0 (no additive defect with *pob3-Q308K*) to 6 (severe additive defect or lethal). No changes were noted for the Spt$^-$ phenotype, which is already severe for *pob3-Q308K* mutants. The combined synthetic defect (SD Severity) was calculated by summing the scores for the Ts$^-$ and HU phenotypes. These scores were used to assign each mutation into mild, moderate, or severe defect classes for use in Figs. 1 and 5.

WT sequence	1st residue	Mutant	Phenotype, Spt$^-$	Phenotype with *pob3-Q308K*				
				HUs	Ts$^-$	Spt$^-$	SD severity	Severity group
			0	0	0	6	0	
SNAEN	39	KNDKK	1	0	1	6	1	Mild
YQK	45	DDD	0	2	3	6	5	Moderate
QRNNK	104	DDDDD	2	3	2	6	5	Moderate
IDIS	163	DRID	0	0	1	6	1	Mild
LKIT	210	DDID	0	1	2	6	3	Mild
NYKFN	245	KDDFD	0	4	3	6	7	Moderate
NYKFN	245	KADFD	0	4	3	6	7	Moderate
YS	257	DD	2	5	5	6	10	Severe
IIQ	260	DIR	3	6	6	6	12	Severe
I	260	D		4	5	6	9	Severe
Q	262	R		1	2	6	3	Mild
DLR	268	KDD	2	5	4	6	9	Severe
L	269	D	1	4	5	6	9	Severe
VSARS	271	DDDDD	2	5	5	6	10	Severe
V	271	D		3	3	6	6	Moderate
QLYGN	279	DLDGR	0	1	1	6	2	Mild
S	289	D		1	3	6	4	Moderate
KPGR	333	DPGD	4	3	3	6	6	Moderate
KN	362	DR	0	0	2	6	2	Mild
EFR	371	AAA	0	1	3	6	4	Moderate
Q	415	R		1	3	6	4	Moderate
Q	415	A		0	1	6	1	Mild
DETE	425	KKKK	0	3	3	6	6	Moderate
AKSQ	439	DDDA	0	4	3	6	7	Moderate

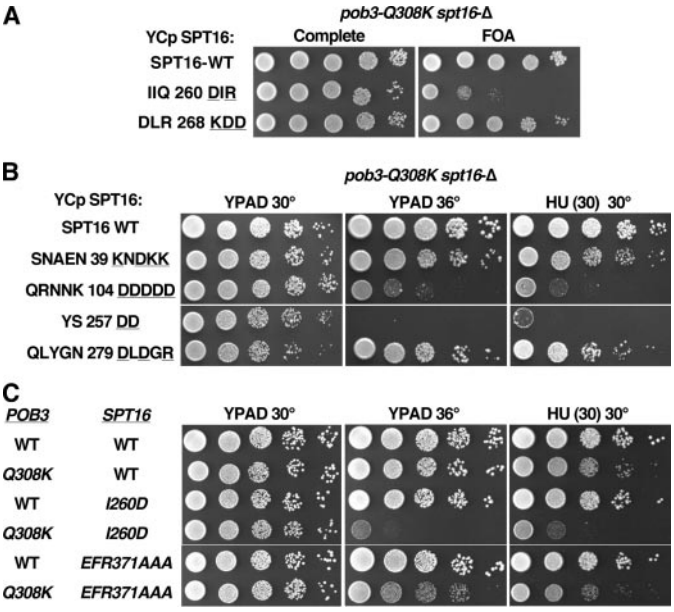

FIGURE 4. **Spt16 NTD point mutations cause synthetic defects with *pob3-Q308K*.** *A*, strain 8319-2-4 (A364a background, *spt16-Δ pob3-Q308K*) carrying a low copy plasmid with the *SPT16* and *URA3* genes was transformed with low copy plasmids carrying the alleles of *SPT16* indicated and the *LEU2* gene. Transformants were grown in medium lacking leucine and then tested on plates containing 5-FOA as in Fig. 3. Poor growth on 5-FOA indicates that the *spt16-IIQ260DIR pob3-Q308K* combination is viable but incapacitated. This allele of *SPT16* supports normal growth in a WT *POB3* strain (Table 2 and supplemental material). *B*, as in *A*, except strains were recovered after treatment with 5-FOA, grown to saturation in rich medium, and then tested on YPAD or YPAD with 30 mM HU at the temperatures indicated. *2nd* and *5th rows* are examples of mild synthetic defects with *pob3-Q308K* (Table 2); *3rd row* is and example of a moderate defect, and the *4th row* is an example of a severe defect. *C*, selected mutations were integrated into the genome (A364a background) and then crossed to a strain with the *pob3-Q308K* mutation. Single and double mutants (8127-5-2, 8324-1-4, 8364-I260D-2d, 8364-I260D-1c, 8364-371-8b, and 8364-371-7c) were diluted and tested as in *B*.

retested to determine the importance of individual residues. For example, IIQ 260 DIR was essentially lethal when combined with *pob3-Q308K*, and the I260D mutation was found to contribute more to this defect than Q262R (Table 2 and Fig. 4*C*). Western blotting was also used to show that these point mutations in Spt16 did not significantly destabilize Spt16 or Pob3 proteins in either *POB3* or *pob3-Q308K* strains (supplemental Fig. S4).

Combining mutations in the Spt16 NTD with *pob3-Q308K* therefore caused a range of effects from no added defect to near lethality. The severity of the synthetic defect is rated in Table 2 and mapped to the structure in Fig. 5. Importantly, the strongest synthetic defects are caused by mutations in residues within the putative peptide binding cleft and tunnel. We conclude that this region is important for performing the role of the Spt16 NTD that functionally overlaps with Pob3-M.

Spt16 NTD Does Not Bind N-terminal Tails of Histones—The four histone proteins all have N-terminal tails that extend beyond the structured core of the nucleosome (47). The similarity of the Spt16 NTD to peptide-binding proteins suggested the obvious possibility that these tails are the substrate for binding by the Spt16 NTD. We tested this idea genetically by looking for interactions between *spt16-ΔNTD* and mutations in the histone tails. Weak interactions consistent with a role of yFACT in nucleosome deposition were observed, but overall the pattern of interactions was not consistent with a direct role for the Spt16 NTD as the binding module for histone tails (supplemental Materials and supplemental Fig. S5). We also asked whether the Spt16 NTD binds to histone tails *in vitro* using several different strategies. In one approach, we found that the N-terminal tails of histones are an important component of the interaction between yFACT and nucleosomes, because nucleosomes treated with trypsin to remove the tails were no longer able to bind to yFACT (Fig. 6*A*). However, yFACT complexes lacking the Spt16 NTD, with a Pob3-Q308K mutation or with both defects, were able to bind to nucleosomes without a decrease in affinity (Fig. 6*B*). These mutated proteins were also able to produce the same increase in accessibility of nucleosomal DNA to nucleases observed with WT proteins (Fig. 6*C*). Finally, yFACT was found to bind to synthetic histone peptides with high affinity using a surface plasmon resonance assay, but the purified Spt16 NTD did not have this activity, and an Spt16-ΔNTD-Pob3 complex lacking the Spt16 NTD retained the ability to bind to peptides (Fig. 6*D*). We were therefore unable to obtain evidence to support the hypothesis that histone N-terminal tails are bound by the Spt16 NTD, although the tails of at least H3 and H4 are bound by some component of yFACT in an interaction that is important for yFACT function.

The H2A C-terminal Extension Is Important for yFACT Function—The specific structural changes that occur during yFACT-mediated nucleosome reorganization are not known, but it has been suggested that H2A-H2B dimers might be partially or fully displaced (8). Nuclease sensitivity results are not consistent with a simple displacement model (1, 7); however, it remains likely that altered contacts among histone proteins within the octamer core contribute to the changes produced by yFACT. Because the N-terminal histone tails do not appear to be the substrate for binding by the Spt16 NTD or the region of Pob3-M disturbed by the Pob3-Q308K mutation, we examined the nucleosome structure for other candidate regions whose structure might be altered if H2A-H2B dimer contacts with $(H3\text{-}H4)_2$ tetramers were broken. Aside from the unstructured N-terminal tails, most of H2B, H3, and H4 exhibit independent tertiary structural organization. In contrast, the C-terminal region of H2A (roughly residues 107–132) extends beyond the globular histone fold region to traverse the surface of the $(H3\text{-}H4)_2$ tetramer (Fig. 7). All but the last 6 residues are ordered in one monomer of the published crystal structure of the yeast nucleosome (27), but because this extended "docking" region of H2A makes extensive contacts with tetramers, it is likely to be unstructured in free H2A-H2B dimers. This stirrup-like domain contributes a large fraction of the buried surface area between H2A-H2B dimers and $(H3\text{-}H4)_2$ tetramers (27), and it has been shown to be important in preventing dissociation of dimers and sliding of nucleosomes (26, 28). This region of H2A is therefore a strong candidate for a domain that would be important for factors like yFACT that modulate nucleosome stability.

We therefore tested for genetic interactions between yFACT mutations and mutations in the H2A docking domain. We compared four strains, each with a single *URA3*-marked plasmid as the only source of histone genes. The strains were otherwise either WT or had the single additional genomic muta-

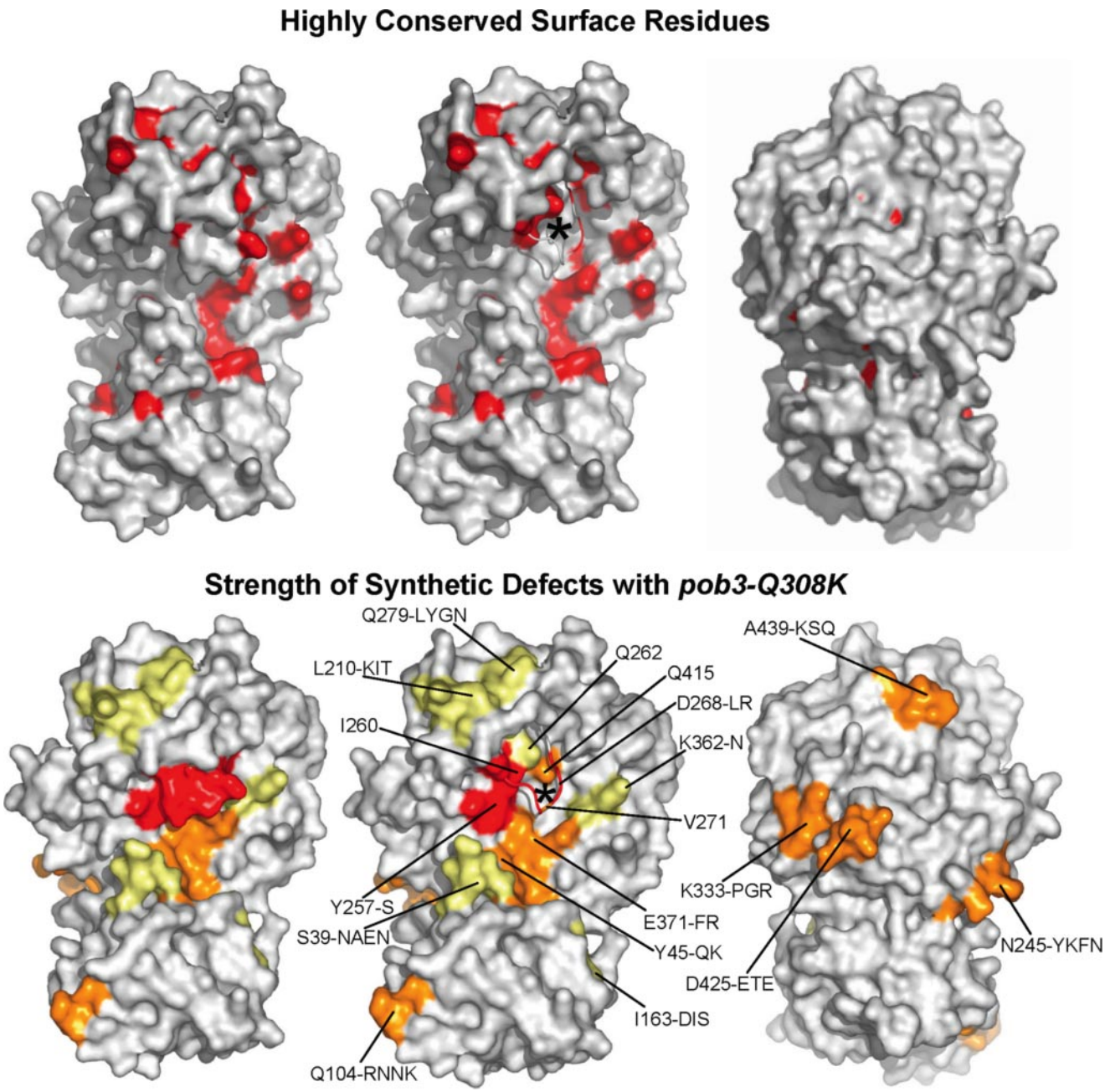

FIGURE 5. **Conservation correlates with the strength of synthetic defects with *pob3-Q308K*.** *Top,* residues that are identical among at least 70% of the 31 Spt16 homologs aligned (see Fig. 1) are indicated in *red*, revealing clustering near the canonical binding/active site cleft for prolidase, methionine aminopeptidase, aminopeptidase P, and creatinase (*asterisk*). The full surface is shown on the *left*, and the loop residues 266–274 are removed in the *middle panel* to reveal the enclosed tunnel region. The *right panel* shows a view rotated 180° about the *vertical axis*. *Bottom,* severity of the synthetic defect when combined with *pob3-Q308K* is indicated (Table 2); severe defects are shown in *red*, moderate defects in *orange*, and mild defects in *yellow*. If residues were tested individually and in multiple mutations, only the score from the single mutation is used here. Otherwise, the score for the complex mutation is assigned to all residues altered. WT sequences are indicated along with the number of the first residue. The orientations are the same as in the *top panels*.

tions *pob3-Q308K*, *spt16-ΔNTD*, or *spt16-11*. The latter allele carries two mutations in the Spt16-M domain (6) and causes strong HU sensitivity, temperature sensitivity, and the Spt$^-$ phenotype, much stronger defects than those caused by *spt16-ΔNTD*. This strain serves as a control to ask whether effects are specific to mutations that alter the putative binding motifs found in Pob3-M and the Spt16 NTD, or are instead general phenotypes associated with yFACT defects. The four strains were transformed with plasmids expressing the normal H2B, H3, and H4 proteins, but expressing a mutant H2A protein. The ability to lose the fully WT histone plasmid was determined by plating on medium containing 5-FOA to select for loss of the *URA3*-marked WT plasmid. Both WT and *spt16-11* strains were able to tolerate G107S, L109S, and H113R mutations in H2A (Fig. 7). In contrast, H2A-G107S could not support viability in either a *pob3-Q308K* strain or an *spt16-ΔNTD* strain (Fig. 7). H2A-H113R also could not support viability in a *pob3-Q308K* strain, but this mutation was not detrimental for the growth of an *spt16-ΔNTD* strain. These tests show that mutations that disturb potential binding domains of yFACT require

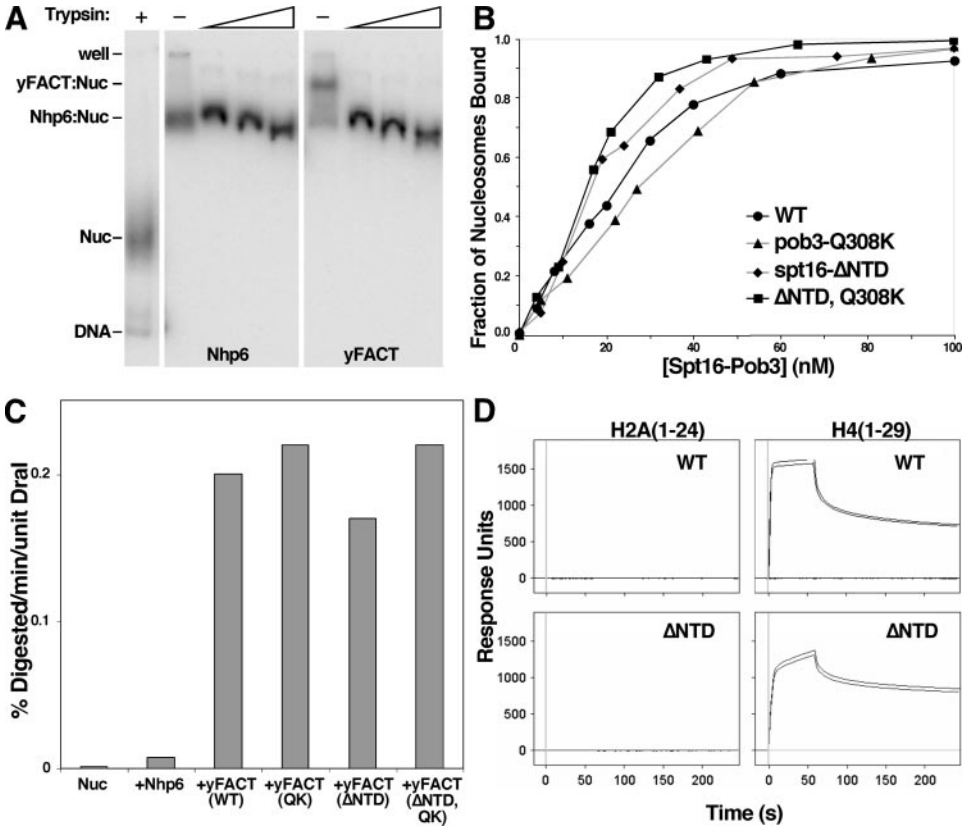

FIGURE 6. **Tests for features important to the direct interaction between yFACT and nucleosomes.** *A,* histone tails contribute to yFACT binding to nucleosomes (*Nuc*). Nucleosomes were reconstituted *in vitro* (supplemental Methods) and then treated with increasing amounts of trypsin, followed by addition of a protease inhibitor. Samples were mixed with Nhp6 or yFACT proteins as indicated then separated by native PAGE. Nhp6 bound to the nucleosomes normally even at the highest level of trypsin digestion, but even the lowest level of trypsin used blocked formation of yFACT-nucleosome complexes. *B,* mutation of putative peptide binding domains does not inhibit yFACT interaction with nucleosomes. Binding of yFACT to nucleosomes was measured using the electrophoretic mobility shift in native polyacrylamide gels, as in *A*. Spt16-Pob3 complexes were titrated using saturating levels of Nhp6, and the percentage of the nucleosomes shifted to the slower migrating form characteristic of complex formation was determined by phosphorimaging. WT (Spt16-Pob3), ΔNTD (Spt16-ΔNTD-Pob3), Q308K (Spt16-Pob3-Q308K), and the double mutant were compared in the same experiment. The concentration of each complex was determined by comparing the amount of intact Pob3 by Coomassie Blue staining after SDS-PAGE and by absorbance at 280 nm; the variability in determining the concentration of intact Spt16-Pob3 was in the range of the small differences in affinity observed here. The affinity was reproducibly slightly higher for complexes lacking the Spt16 NTD. It is therefore clear that deletion of the Spt16 NTD did not decrease the affinity of yFACT for nucleosomes, but we cannot conclude that this does not cause a slight increase in the affinity. *C,* mutation of yFACT does not alter the ability to increase accessibility to restriction endonucleases. The same four protein complexes used in *B* were tested for the ability to enhance digestion by DraI. In each case, the initial rate of digestion was determined by plotting multiple time points and then converted to a rate corrected for the amount of enzyme added as described previously (7). All four complexes displayed equivalent accessibility, indicating that neither the pob3-Q308K mutation nor the deletion of the NTD of Spt16 prevent yFACT from promoting this change in nucleosomes. Similar results were obtained with a different positioning sequence and the enzyme PstI (48; data not shown). *D,* N-terminally biotinylated synthetic peptides representing residues 1–24 of H2A or 1–29 of H4 were immobilized on a streptavidin chip, and binding of WT or Spt16-ΔNTD-Pob3 complexes was detected using surface plasmon resonance in two sequential tests. Binding to H4-(1–29) was complex and could not be fit to simple binding kinetics, but both complexes were able to bind an H4 tail peptide but not an H2A tail peptide. The NTD therefore may influence H4 tail peptide binding by yFACT, but is not required for it. Binding was also detected using an H3 tail peptide (data not shown).

nucleosomes to have normal features in the H2A docking domain. The H2A-G107S mutation was detrimental to an *spt16-11* strain, but this combination was viable, indicating that the requirement for a normal H2A docking domain is at least somewhat specific for yFACT mutations that alter potential binding motifs. Furthermore, Pob3-M and Spt16 NTD mutants require overlapping but distinct features to remain unperturbed within the H2A docking domain, consistent with their overlapping but distinct roles in promoting some essential function, as revealed by their distinct phenotypes when tested alone but synthetic lethality when combined (Fig. 3). These results suggest that the docking domain of H2A plays an important role in yFACT-mediated nucleosome reorganization and that the potential binding sites in the Pob3-M and Spt16 N-terminal domains functionally overlap to perform this role. Several possible functions for these domains are discussed below.

DISCUSSION

FACT homologs alter the properties of nucleosomes in a way that is important for transcription and replication, and this change is likely to include altered contacts between H2A-H2B dimers and $(H3\text{-}H4)_2$ tetramers (1, 7, 8, 13). Genetic interactions between yFACT and the Hir-Hpc complex suggest that a normal cycle of reorganization usually includes restoration of normal nucleosome structure after providing increased accessibility to the nucleosomal DNA (13). In this view, yFACT alters a nucleosome, tethers the components together, and then returns them to their initial state. We have shown that the Spt16 NTD and the Pob3-M domain each form potential binding surfaces, and that these sites are functionally redundant for some essential role of yFACT. Our analysis shows that yFACT complexes lacking normal versions of these sites cannot support viability but can still effect nucleosome reorganization *in vitro*. It is therefore likely that the potential binding sites act during the tethering or restoration phases of the reorganization cycle, rather than during initiation of reorganization.

The N-terminal tails of the histones appear to be important during an early stage of reorganization, because nucleosomes lacking these peptides are not bound efficiently by yFACT. Our data do not support a role for the potential binding sites in Pob3-M or the Spt16 NTD in binding these N-terminal tails, so the interaction with the N-terminal histone tails appears to be mediated by other regions of yFACT yet to be defined. However, we find that the stirrup-like C-terminal extension or docking domain of H2A has a role in reorganization that functionally overlaps both Pob3-M and the Spt16 NTD, as any combination of double

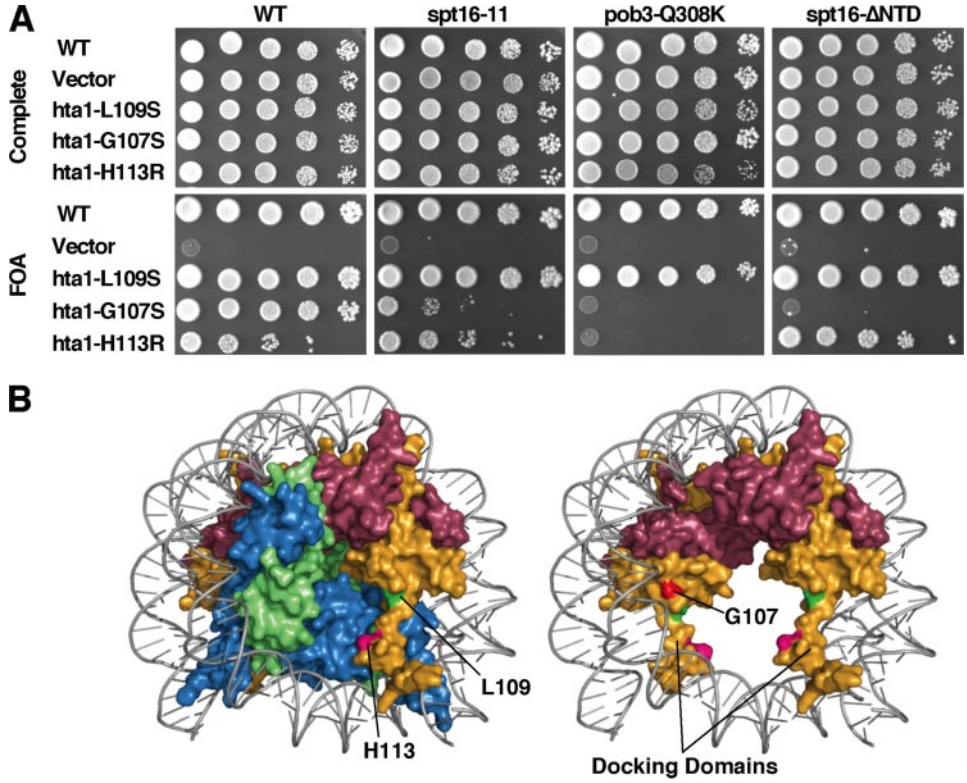

FIGURE 7. **The H2A docking domain is important during yFACT function.** *A,* strains DY9999, DY10003, 8264-17-3, and 8407-10-2 with the genotypes indicated and lacking genomic histone genes but carrying a low copy *URA3* plasmid with all four histone genes were transformed with low copy plasmids with the H2A mutations indicated. Cultures were tested on synthetic complete medium or medium containing 5-FOA as in Fig. 3. *B,* locations of H2A residues mutated in *A* are shown on the yeast nucleosome (PDB 1ID3; 27) Gly-107 is shown in *red*, Leu-109 in *green*, and His-113 in *magenta*. The remainder of H2A is *orange*; H2B is *purple*; H3 is *blue*; and H4 is *green*. The nucleosome is intact in the *left panel* and H3 and H4 are removed in the *right panel* to show Gly-107, which is buried in the docking interface, and to emphasize the stirrup-like extension of the docking domains away from the globular domains of H2A-H2B dimers.

mutants within this set is lethal. Interaction between the H2A docking domain and $(H3\text{-}H4)_2$ tetramers is important for preventing H2A-H2B dimer dissociation and nucleosome sliding (28), making this an interface that is likely to be important for yFACT functions. We therefore consider several models for how the H2A docking domain could be involved in reorganization that are consistent with our results.

First, the H2A docking domain could act during an early step. For example, reorganization by yFACT could be initiated by breaking contacts between the H2A docking domain and the $(H3\text{-}H4)_2$ tetramer surface as this would facilitate rearrangement of the histone core and/or displacement of H2A-H2B dimers. Our results do not address a role in this step because Spt16-ΔNTD-Pob3-Q308K complexes bind to and reorganize nucleosomes normally. However, this model makes specific predictions regarding the mechanism of reorganization that can now be tested.

Second, the H2A docking domain could act to tether nucleosomal components together during reorganization. In one model, contact between Pob3-M and some part of the histone core, between the Spt16 ΔNTD and another part of the histone core, and between the H2A docking domain and $(H3\text{-}H4)_2$ tetramers all contribute independently to maintaining contact among the components of the nucleosome during reorganization. The synthetic lethality observed between any pair of mutations would then be explained if any two points of contact are sufficient to prevent intolerable amounts of nucleosome damage from occurring, but one point of contact is not.

Third, the H2A docking domain could pose a barrier to restoration of nucleosome structure, requiring a chaperone to make insertion of H2A-H2B dimers more efficient. In this model, the H2A docking domain becomes disordered during reorganization because it is no longer in contact with the $(H3\text{-}H4)_2$ tetramer. Restoration of the normal nucleosome therefore requires positioning of this region in a conformation compatible with the docking interaction. The potential binding sites in Pob3-M and the Spt16 NTD could either act as redundant chaperones that can each promote this conformation or each could contribute independently to this outcome. In either case, The H2A-G107S mutation could make it more difficult to achieve the appropriate shape, making loss of either binding site/chaperone lethal.

Many other related models can be imagined. The identification of specific potential roles for domains of yFACT and for features of nucleosomes allows us to make more rigorous, experimentally testable predictions about the mechanism of yFACT-mediated nucleosome reorganization. The insight provided by the structural, genetic, and biochemical results reported here therefore allows us to begin a more detailed analysis of this important component of chromatin-mediated processes.

Acknowledgments—We thank Mary Blanksma, Aileen Olsen, Susan Ruone, and Elliot Ferris for technical assistance; Brad Cairns for histone peptides; Greg Pratt, Xiaolin Gao, and Martin Rechsteiner for protease assays; Dennis Winge for metal analysis; and David Myszka for SPR analysis. Operations of the National Synchrotron Light Source are supported by the United States Department of Energy, Office of Basic Energy Sciences, and by the National Institutes of Health. Data collection at the National Synchrotron Light Source was funded by the National Center for Research Resources.

REFERENCES

1. Ruone, S., Rhoades, A. R., and Formosa, T. (2003) *J. Biol. Chem.* **278,** 45288–45295
2. Singer, R. A., and Johnston, G. C. (2004) *Biochem. Cell Biol.* **82,** 419–427
3. Orphanides, G., Wu, W. H., Lane, W. S., Hampsey, M., and Reinberg, D. (1999) *Nature* **400,** 284–288
4. De Koning, L., Corpet, A., Haber, J. E., and Almouzni, G. (2007) *Nat. Struct. Mol. Biol.* **14,** 997–1007

5. Biswas, D., Yu, Y., Prall, M., Formosa, T., and Stillman, D. J. (2005) *Mol. Cell. Biol.* **25,** 5812–5822
6. Formosa, T., Eriksson, P., Wittmeyer, J., Ginn, J., Yu, Y., and Stillman, D. J. (2001) *EMBO J.* **20,** 3506–3517
7. Rhoades, A. R., Ruone, S., and Formosa, T. (2004) *Mol. Cell. Biol.* **24,** 3907–3917
8. Reinberg, D., and Sims, R. J., III (2006) *J. Biol. Chem.* **281,** 23297–23301
9. Malone, E. A., Clark, C. D., Chiang, A., and Winston, F. (1991) *Mol. Cell. Biol.* **11,** 5710–5717
10. Rowley, A., Singer, R. A., and Johnston, G. (1991) *Mol. Cell. Biol.* **11,** 5718–5726
11. Kaplan, C. D., Laprade, L., and Winston, F. (2003) *Science* **301,** 1096–1099
12. Budd, M. E., Tong, A. H., Polaczek, P., Peng, X., Boone, C., and Campbell, J. L. (2005) *Plos Genet.* **1,** e61
13. Formosa, T., Ruone, S., Adams, M. D., Olsen, A. E., Eriksson, P., Yu, Y., Rhoades, A. R., Kaufman, P. D., and Stillman, D. J. (2002) *Genetics* **162,** 1557–1571
14. Gambus, A., Jones, R. C., Sanchez-Diaz, A., Kanemaki, M., van Deursen, F., Edmondson, R. D., and Labib, K. (2006) *Nat. Cell Biol.* **8,** 358–366
15. Hertel, L., De Andrea, M., Bellomo, G., Santoro, P., Landolfo, S., and Gariglio, M. (1999) *Exp. Cell Res.* **250,** 313–328
16. O'Donnell, A. F., Brewster, N. K., Kurniawan, J., Minard, L. V., Johnston, G. C., and Singer, R. A. (2004) *Nucleic Acids Res.* **32,** 5894–5906
17. Okuhara, K., Ohta, K., Seo, H., Shioda, M., Yamada, T., Tanaka, Y., Dohmae, N., Seyama, Y., Shibata, T., and Murofushi, H. (1999) *Curr. Biol.* **9,** 341–350
18. Schlesinger, M. B., and Formosa, T. (2000) *Genetics* **155,** 1593–1606
19. Wittmeyer, J., Joss, L., and Formosa, T. (1999) *Biochemistry* **38,** 8961–8971
20. Zhou, Y., and Wang, T. S. (2004) *Mol. Cell. Biol.* **24,** 9568–9579
21. Lejeune, E., Bortfeld, M., White, S. A., Pidoux, A. L., Ekwall, K., Allshire, R. C., and Ladurner, A. G. (2007) *Curr. Biol.* **17,** 1219–1224
22. Zipperlen, P., Fraser, A. G., Kamath, R. S., Martinez-Campos, M., and Ahringer, J. (2001) *EMBO J.* **20,** 3984–3992
23. VanDemark, A. P., Blanksma, M., Ferris, E., Heroux, A., Hill, C. P., and Formosa, T. (2006) *Mol. Cell* **22,** 363–374; Correction (2007) *Mol. Cell* **27,** 171–172
24. Aravind, L., and Koonin, E. V. (1998) *Curr. Biol.* **8,** R111–R113
25. Biswas, D., Dutta-Biswas, R., Mitra, D., Shibata, Y., Strahl, B. D., Formosa, T., and Stillman, D. J. (2006) *EMBO J.* **25,** 4479–4489
26. Park, Y. J., Dyer, P. N., Tremethick, D. J., and Luger, K. (2004) *J. Biol. Chem.* **279,** 24274–24282
27. White, C. L., Suto, R. K., and Luger, K. (2001) *EMBO J.* **20,** 5207–5218
28. Ferreira, H., Somers, J., Webster, R., Flaus, A., and Owen-Hughes, T. (2007) *Mol. Cell. Biol.* **27,** 4037–4048
29. Van Duyne, G. D., Standaert, R. F., Karplus, P. A., Schreiber, S. L., and Clardy, J. (1993) *J. Mol. Biol.* **229,** 105–124
30. Otwinowski, Z., and Minor, W. (1996) *Methods Enzymol.* **276,** 307–326
31. Terwilliger, T. C., and Berendzen, J. (1999) *Acta Crystallogr. Sect. D Biol. Crystallogr.* **55,** 849–861
32. Terwilliger, T. C. (2003) *Acta Crystallogr. Sect. D Biol. Crystallogr.* **59,** 38–44
33. McCoy, A. J., Grosse-Kunstleve, R. W., Storoni, L. C., and Read, R. J. (2005) *Acta Crystallogr. Sect. D Biol. Crystallogr.* **61,** 458–464
34. Emsley, P., and Cowtan, K. (2004) *Acta Crystallogr. Sect. D Biol. Crystallogr.* **60,** 2126–2132
35. Collaborative Computational Project, No. 4 (1994) *Acta Crystallogr. Sect. D Biol. Crystallogr.* **50,** 760–763
36. Painter, J., and Merritt, E. A. (2006) *J. Appl. Crystallogr.* **39,** 109–111
37. Burke, D., Dawson, D., and Stearns, T. (2000) *Methods in Yeast Genetics: A Cold Spring Harbor Laboratory Course Manual*, Cold Spring Harbor Laboratory Press, Cold Spring Harbor, NY
38. Ariyoshi, M., Vassylyev, D. G., Iwasaki, H., Nakamura, H., Shinagawa, H., and Morikawa, K. (1994) *Cell* **78,** 1063–1072
39. Coll, M., Knof, S. H., Ohga, Y., Messerschmidt, A., Huber, R., Moellering, H., Russmann, L., and Schumacher, G. (1990) *J. Mol. Biol.* **214,** 597–610
40. Padmanabhan, B., Paehler, A., and Horikoshi, M. (2002) *Acta Crystallogr. Sect. D Biol. Crystallogr.* **58,** 1322–1328
41. Kowalinski, E., Bange, G., Bradatsch, B., Hurt, E., Wild, K., and Sinning, I. (2007) *FEBS Lett.* **581,** 4450–4454
42. Monie, T. P., Perrin, A. J., Birtley, J. R., Sweeney, T. R., Karakasiliotis, I., Chaudhry, Y., Roberts, L. O., Matthews, S., Goodfellow, I. G., and Curry, S. (2007) *EMBO J.* **26,** 3936–3944
43. Maher, M. J., Ghosh, M., Grunden, A. M., Menon, A. L., Adams, M. W., Freeman, H. C., and Guss, J. M. (2004) *Biochemistry* **43,** 2771–2783
44. Roderick, S. L., and Matthews, B. W. (1993) *Biochemistry* **32,** 3907–3912
45. Simchen, G., Winston, F., Styles, C. A., and Fink, G. R. (1984) *Proc. Natl. Acad. Sci. U. S. A.* **81,** 2431–2434
46. Boeke, J. D., Trueheart, J., Natsoulis, G., and Fink, G. R. (1987) *Methods Enzymol.* **154,** 164–175
47. Luger, K., Mader, A. W., Richmond, R. K., Sargent, D. F., and Richmond, T. J. (1997) *Nature* **389,** 251–260
48. Fan, H. Y., He, X., Kingston, R. E., and Narlikar, G. J. (2003) *Mol. Cell* **11,** 1311–1322